

Vibrational modes of negatively charged silicon-vacancy centers in diamond from *ab initio* calculations

Elisa Londero,¹ Gergő Thiering,^{1,2} Adam Gali,^{1,2,*} and Audrius Alkauskas^{3,†}

¹*Institute for Solid State Physics and Optics, Wigner Research Centre for Physics, Hungarian Academy of Sciences, P.O. Box 49, Budapest H-1525, Hungary*

²*Department of Atomic Physics, Budapest University of Technology and Economics, Budapest H-1111, Hungary*

³*Center for Physical Sciences and Technology, Vilnius LT-10257, Lithuania*

(Dated: November 28, 2018)

Silicon-vacancy (SiV) center in diamond is a photoluminescence (PL) center with a characteristic zero-phonon line energy at 1.681 eV that acts as a solid-state single photon source and, potentially, as a quantum bit. The majority of the luminescence intensity appears in the zero-phonon line; nevertheless, about 30% of the intensity manifests in the phonon sideband. Since phonons play an important role in the operation of this system, it is of importance to understand the vibrational properties of the SiV center in detail. To this end, we carry out density functional theory calculations of dilute SiV centers by embedding the defect in supercells of a size of a few thousand atoms. We find that there exist two well-pronounced quasi-local vibrational modes (resonances) with a_{2u} and e_u symmetries, corresponding to the vibration of the Si atom along and perpendicular to the defect symmetry axis, respectively. Isotopic shifts of these modes explain the isotopic shifts of prominent vibronic features in the experimental SiV PL spectrum. Moreover, calculations show that the vibrational frequency of the a_{2u} mode increases by about 25% in the excited state with respect to the ground state, while the frequency of the e_u mode increases only slightly. These changes explain experimentally observed isotopic shifts of the zero-phonon line energy. We also emphasize possible dangers of extracting isotopic shifts of vibrational resonances from finite-size supercell calculations, and instead propose a method to do this efficiently.

I. INTRODUCTION

The study of optically active paramagnetic defects in diamond has a rich history¹. In the past two decades or so, nitrogen-vacancy (NV) centers attracted a lot of attention due to their potential applications in a variety of emerging *quantum technologies*, e.g., as spin qubits, sensors, or single-photon emitters². More recently, the diamond silicon-vacancy (SiV) center has been demonstrated as a single photon source^{3,4}. In pure diamond samples the zero-phonon-line (ZPL) of the SiV center is at 1.681 eV, thus, in the infra-red region. The defect is a $S = 1/2$ center and it can be coherently manipulated optically at a single-site level⁵. Earlier studies indicated that the SiV center is negatively charged and that the Si atom resides in the symmetric split-vacancy configuration that exhibits D_{3d} symmetry⁶ (Fig. 1), with defect oriented along the $\langle 111 \rangle$ axis. *Ab initio* calculations found that the optical signal of the defect can be described by the transition between e_u and e_g defect states⁷. Both the ground 2E_g (electronic configuration $e_u^4 e_g^3$) and the excited 2E_u ($e_u^3 e_g^4$) states are dynamic Jahn-Teller (JT) systems^{8,9} that preserve the high D_{3d} symmetry.

Like for other defects, lattice vibrations play an important role in defining many properties of SiV centers. Most prominently, this concerns optical properties: while luminescence of SiV centers is mainly dominated by the ZPL transition with $\sim 70\%$ of the total emission, the remaining $\sim 30\%$ show up in the phonon sideband with a few distinct phonon replicas¹⁰. In a recent study one of those replicas, occurring at 64 meV from the ZPL energy

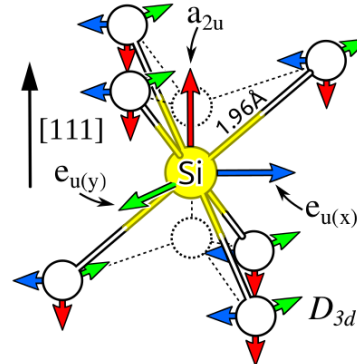


FIG. 1. (color online) The geometry sketch of the SiV center. The localized vibration modes e_u (motion of Si-atom perpendicular to $\langle 111 \rangle$ axis: green and blue arrows) and a_{2u} (motion of Si-atom parallel to $\langle 111 \rangle$ axis: red arrow) are also shown. These quasi-local vibration modes have significant localization on the six neighbor carbon atoms that move in the opposite direction to that of Si atom in the corresponding vibrations.

and having a relative intensity of $\sim 3\%$ w.r.t. the ZPL, was shown to exhibit an isotope shift that was proportional to the inverse square-root of the silicon mass for three different Si isotopes (^{28}Si , ^{29}Si , ^{30}Si)¹¹. In absolute units, downward shifts for ^{29}Si and ^{30}Si isotopes were 8.22 cm^{-1} (1.02 meV) and 17.81 cm^{-1} (2.21 meV). Earlier density functional theory (DFT) calculations¹² indeed found a quasi-local mode with similar energy (56.45 meV), but with significantly smaller calculated shifts of

5 and 10 cm⁻¹, respectively, calling for a deeper analysis of quasi-local SiV vibrations. Phonons also play an important role in nonradiative processes in defects. It is known that quantum efficiency of optical emission at SiV centers most likely does not exceed 20 %, indicating the existence of detrimental non-radiative decay channels¹³. Therefore, phonons affect or govern both radiative and non-radiative processes at SiV centers, but a deeper understanding of them is currently missing. In this paper, we report *ab initio* density functional theory (DFT) calculations of vibrational modes of effectively isolated SiV(–) in both ground and excited states. Calculations are accompanied by the group theory analysis of the phonon spectrum of the SiV center. Our findings explain a few recent experimental observations. Also, they solve the apparent contradiction of the results reported in Ref. 12 and recent experiments.

The paper is organized as follows. In Sec. II we present the details of DFT calculations, including the electronic structure methods, calculations of vibrational modes, and analysis of vibrations. In Sec. III we present the results of calculations of vibrations in the ground state, as well as discuss isotopic shifts of phonon modes. In Sec. IV the results for the excited electronic state are presented. In Sec. V we discuss our calculations in light of experiments and highlight remaining unanswered questions. Finally, in Sec. VI we summarize our work and draw conclusions.

II. METHODOLOGY

A. Electronic structure and vibrational spectra

Ab initio calculations employed in the current work were similar to a previous study⁷. In short, we determined the electronic structure of the SiV(–) center within the framework of DFT as implemented in the VASP code¹⁴. We used the hybrid Heyd-Scuseria-Ernzerhof functional¹⁵ HSE06 (HSE for short) with a standard fraction of screened Fock exchange $a = 0.25$ to describe the electronic structure. Lattice constant $a = 3.544$ Å and the band gap $E_g = 5.3$ eV are in excellent agreement with experimental values. The use of a hybrid functional for the SiV center is especially important to describe the excited state⁷. However, for the vibrational properties of the ground state we have also in addition employed calculations based on the computationally significantly cheaper semi-local density functional or Perdew, Burke, and Ernzerhof¹⁶, as discussed in more detail below. Interactions between valence electrons and ions were treated via the projector-augmented wave approach¹⁴. A kinetic-energy cutoff of 400 eV was used for a plane-wave expansion of wavefunctions. The Brillouin zone was sampled at the Γ point, and this choice was made in order to make sure that the local symmetry is correctly described. We used both 216- and 512-atom cubic supercells for defect calculations¹⁷. The 2E_u excited state was calculated by

the constrained-DFT method (originally due to Slater¹⁸, see Ref. 19 for a review of new developments), whereby the electron is promoted from the e_u level to the e_g defect level. The methodology was previously applied to the NV center in diamond²⁰, where a very good agreement with experiment was demonstrated.

The HSE functional provides an accurate description of both the geometry and the electronic structure of the SiV(–) center⁷. The calculated ZPL energy for the transition $^2E_g \rightarrow ^2E_u$ of 1.72 eV compares very favorably with the experimental value of 1.681 eV⁷. Thus, it is desirable to also calculate vibrations at the hybrid functional level. However, this is prohibitively costly even for the 216-atom supercell. To calculate the vibrational of HSE-quality in very large supercells (essentially dilute limit) we use the following methodology.

First, the vibrational spectra for supercells containing 216 or 512 atoms were determined by direct diagonalization of the dynamical matrix computed completely from first principles at the PBE level. Then the calculations were repeated using an embedding procedure previously tested for the NV center in diamond²¹. The procedure relies on the fact that the dynamical matrix is diamond is rather short-ranged, even for charged defects. A modified dynamical matrix was constructed as follows. If two atoms are further away than 4.2 Å then the matrix element is set to zero. Otherwise, if *at least one* of the atoms is closer to the Si atom than 2.75 Å then the dynamical matrix element is taken from the 216-atom PBE calculation. For all other atom pairs we used the value derived from bulk diamond calculations also performed in the 216-atom supercell. In this way we constructed dynamical matrices for 216- and 512-atom supercells. The vibrational frequencies obtained by the full calculation agreed very closely with calculations using the embedding procedure, justifying the use of the latter.

Given the success of the embedding procedure at the PBE level, we performed similar calculations at the HSE level. Here, all matrix elements were taken from the corresponding HSE calculations of the defect (in the ground or the excited state) and bulk diamond. Calculations at the HSE level confirm that PBE provides a very good description of the vibrational spectrum in the ground state. In particular, the agreement between PBE and HSE is better than 2 meV for quasi-local modes (see the discussion below). The largest difference is found in the description of the bulk phonon spectrum. For example, for highest-energy longitudinal optical modes PBE yields 162 meV, while HSE gives 167 meV, that is a bit closer to the experimental value at 165 meV. The HSE spectrum is slightly “stretched” compared to the PBE spectrum. Using the embedding procedure, HSE-level calculations of the vibrational spectrum were calculated for supercells containing up to 4096 atoms. We label supercells $N \times N \times N$, where N is the number of cubic diamond unit cells in any direction. Pristine supercells contain $8N^3$ atoms and thus supercells with $N = 3, 4, 5$, and $6, 7$, and 8 contain the nominal number of atoms $M =$

216, 512, 1000, 1726, 2744, and 4096, respectively. In all calculations of the dynamical matrix we used 0.5 occupations for spin-unpaired e orbitals to avoid complications with the JT effect. In these calculations the actual electronic configurations were $e_{ux}^2 e_{uy}^2 e_{gx}^{1.5} e_{gy}^{1.5}$ for the ground and $e_{ux}^{1.5} e_{uy}^{1.5} e_{gx}^2 e_{gy}^2$ for the excited state.

B. Characterization of phonons

All the vibrational modes have been characterized according to the irreducible representation of the D_{3d} point group: a_{1g} , a_{1u} , a_{2g} , a_{2u} , e_g , and e_u ²². This has been done by calculating matrix elements (scalar products) of the type $(\Delta\mathbf{r}_k, \hat{O}\Delta\mathbf{r}_k)$, where $\Delta\mathbf{r}$ is a short-hand notation for the eigenmode k , and \hat{O} is a symmetry operation. The eigenmode k is described by a vector with components $\Delta r_{k;\alpha i}$, where α labels atoms, and $i = \{x, y, z\}$. For a uniquely determination of the irreducible representation, it is sufficient to consider symmetry operations C_3 (rotation), σ_d (reflection in the plane that contains the symmetry axis) and i (inversion).

The nature of vibrations was characterized also by their localization. A bulk phonon is entirely delocalized and many atoms participate in that particular vibration. Point defects usually change the vibrational structure of a solid. Sometimes, the defect gives rise to a localized vibrational mode with a frequency outside the vibrational spectrum of the host material. However, defects can also induce quasi-local modes. Their frequencies (energies) overlap with the bulk phonon spectrum, and thus they are not strictly localized, but often they give rise to observable spectroscopic signatures. To quantify the localization, vibrational modes corresponding to each irreducible representation (we say below simply “symmetry”) are characterized by the inverse participation ratio (IPR):

$$\text{IPR}_k = \frac{1}{\sum_{\alpha} p_{k;\alpha}^2}, \quad (1)$$

where

$$p_{k;\alpha} = \sum_i \Delta r_{k;\alpha i}^2. \quad (2)$$

The sum in the first equation runs over all atoms α , and, as before, $i = \{x, y, z\}$. IPR essentially describes onto how many atoms the given mode is localized^{21,23}. E.g., when only one atom vibrates in a given mode, $\text{IPR} = 1$. When all M of the supercell vibrate with equal amplitudes, $\text{IPR} = M$. If every-second atom of the supercell vibrates with an equal amplitude, $\text{IPR} = M/2$; etc.

We also find it very convenient to define a localization ratio β_k ²¹:

$$\beta_k = M/\text{IPR}_k = M \sum_{\alpha} p_{k;\alpha}^2. \quad (3)$$

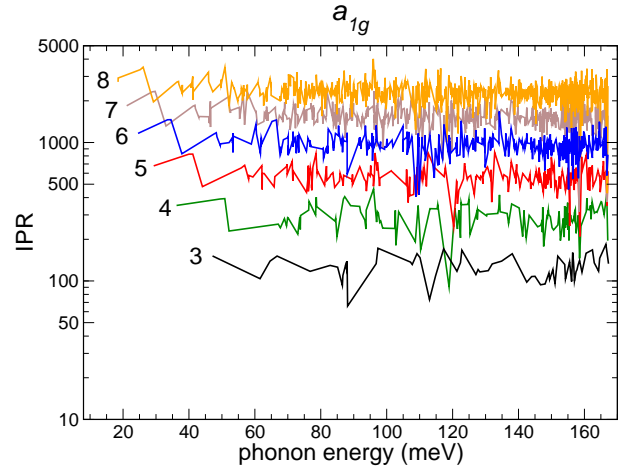


FIG. 2. Inverse participation ratios [Eq. (1)] of a_{1g} symmetry modes for different supercell sizes as a function of energy. Systems with $N = 3, 4, 5, 6, 7, 8$ (size of a cubic supercell, a number next to each graph) correspond to bulk supercells containing $M=8N^3$ atoms. There are no quasi-local modes of a_{1g} symmetry.

β_k quantifies what fraction of atoms in the supercell vibrate for a given vibrational mode k . $\beta_k = 1$ for modes when all atoms in the supercell vibrate with the same amplitude, while $\beta_k \gg 1$ for quasi-localized and local modes.

III. RESULTS: GROUND STATE

We will first focus on the vibrations in the electronic ground state 2E_g . In the current Section we study the ^{28}Si isotope ($m_{\text{Si}} = 28$ a.u.), and leave the study of isotopic shifts to Sec. III C. At the outset, we note that calculations show that there are no truly local vibrational modes with frequencies outside the bulk phonon band. This is expected, as chemical interactions are typically weaker in the vacancy environment and, furthermore, the Si atom is heavier than surrounding carbon atoms. Thus, our subsequent analysis is focused on bulk and quasi-local modes.

A. IPR analysis of the vibration modes

Let us first start with g (even, or *gerade*) modes that are symmetric with respect to inversion. Fig. 2 shows calculated IPRs for fully symmetric a_{1g} modes as a function of energy for different supercell sizes. Physically, a_{1g} represent “breathing” motion with respect to the defect center. We see that for all supercell sizes the IPRs of all vibrational modes are very comparable. In fact, they are all similar to IPRs of bulk modes calculated for the same supercell size. Energies of modes start with the smallest available mode in a given supercell and end with

~ 167 meV.

In principle, quasi-local modes are characterized by IPRs that are noticeably smaller than the average IPR of all the modes in the supercell. Fig. 2 shows that there are no clearly pronounced quasi-local modes of a_{1g} symmetry. IPRs exhibit some variation, but in general we conclude that a_{1g} -symmetry vibrations are just slightly perturbed bulk modes of diamond. The same conclusion holds for modes of a_{2g} symmetry (not shown). In D_{3d} symmetry a_{2g} modes represent rotation motion around the defect axis²². Interestingly, the IPR analysis of e_g modes also shows no indication of the presence of quasi-local e_g modes (not shown). This is an important conclusion, since the dynamic Jahn-Teller effect seen in SiV($-$) centers^{8,9} preserves the inversion symmetry in the ground (as well as the excited state), and, consequently, couples to e_g modes. These modes represent rotation motion around the two axes that are perpendicular to the defect axis. The absence of quasi-local modes of e_g symmetry also shows the complex nature of the Jahn-Teller effect. In order to properly understand it one needs to the coupling to a continuum set of e_g modes²⁴ that are essentially bulk-like. The investigation of the Jahn-Teller effect is beyond the scope of our study.

Thus, *ab initio* calculations show that there are no quasi-local modes of g symmetry and we find only slightly perturbed bulk modes. Since the Si atom is at the center of inversion, Si atom does not participate in even-parity vibrations. We conclude that there are no quasi-local modes (resonances) in which the Si does not move.

Now we turn to the u (uneven, or *ungerade*) modes that break the inversion symmetry. Si atom can contribute to the vibration of these modes. However, IPRs of a_{1u} modes exhibit behavior similar to a_{1g} and other g vibrations (not shown): we find no evidence of quasi-local modes.

The situation is radically different for the a_{2u} modes. In the D_{3d} point group the a_{2u} irreducible representation is special as the z coordinate transforms according to it (z being the symmetry axis). Thus, it can be said that a_{2u} modes are in a way vibrations along the defect axis (see Fig. 1). The IPR analysis is shown in Fig. 3(a). We see a clearly pronounced quasi-local mode with energy $\sim (39 - 49)$ meV where IPRs are significantly smaller than the average IPR for a particular supercell (cf. the situation with a_{1g} modes shown in Fig. 2). A dip happens irrespective of the size of the super-cell. The actual frequencies of vibrational modes with significantly smaller IPRs differ in different supercells, but this is expected due to finite-size effects of the supercells. We also see in Fig. 3(a) that there are no quasi-local modes of a_{2u} symmetry at other energies. Analysis of the vibrational pattern for the quasi-local modes in the energy window $\sim (39 - 49)$ meV shows that in these vibrations it is predominantly the Si-atom that moves along the symmetry axis, as indicated in Fig. 1. The a_{2u} quasi-local mode is analyzed more in Sec. III B.

Calculated IPRs for e_u modes are shown in Fig. 3(b).

The e_u irreducible representation is also special as the $\{x, y\}$ coordinates transform according to it where z is chosen parallel to the symmetry axis, as shown in Fig. 1. Thus, e_u vibrations can be thought as linear motion primarily perpendicular to the defect axis. The IPR analysis indicates that there is quasi-local mode with energies at $\sim (52 - 72)$ meV. Compared to the a_{2u} mode, the e_u resonance is broader, as the decrease of IPRs for the quasi-local mode with respect to delocalized modes is not as significant. The quasi-local vibration mostly corresponds to the Si atom vibrating perpendicular to the defect axis.

The results presented in this Section show that the SiV($-$) induces quasi-local vibrations of a_{2u} and e_u symmetries. In the next Section we analyze these vibrations in more detail.

B. Localization ratios of a_{2u} and e_u modes

For an alternative analysis of quasi-localized modes we use the localization ratio β defined in Eq. (3). The rationale to define β is as follows. For a truly localized phonon mode outside the bulk phonon spectrum IPR is a good quantity to characterize the mode: it converges rather fast as a function of the supercell size, as it acquires a constant value²¹. The situation is different for quasi-local modes. As the size of the supercell increases, IPRs of quasi-local mode increase as well. However, they are always smaller or much smaller than IPRs of bulk modes for a given supercell. This naturally brings to the definition of a relative quantity like the localization ratio β .

Localization ratio for the a_{2u} mode is shown in Fig. 4(a). Different graphs represent calculations from different supercells, and this time they indeed fall on top of each other. For most of the vibrations β fluctuates around a constant value, and we clearly see the emergence of a quasi-local resonance with. The analysis in terms of β is of course only qualitative (β is not a physical quantity that can be measured). However, in Fig. 4(a) we tentatively draw an envelope function to make the reading and understanding of our calculations results clear. This allows us to determine the energy of the a_{2u} quasi-local vibration, about ~ 43 meV. We will provide a more quantitative definition of this energy below.

Analysis for the localization ration of the e_u modes is shown in Fig. 4(b). The emergence of the e_u resonance is clearly seen. As discussed above, the e_u resonance is broader. The energy of the e_u vibration is ~ 60 meV, and it can be seen that the e_u resonance is broader than the a_{2u} resonance.

C. Isotope shifts of the quasi-local a_{2u} and e_u modes

In Ref. 11 it was found that the frequency of vibrational feature in the phonon sideband, which occurs at

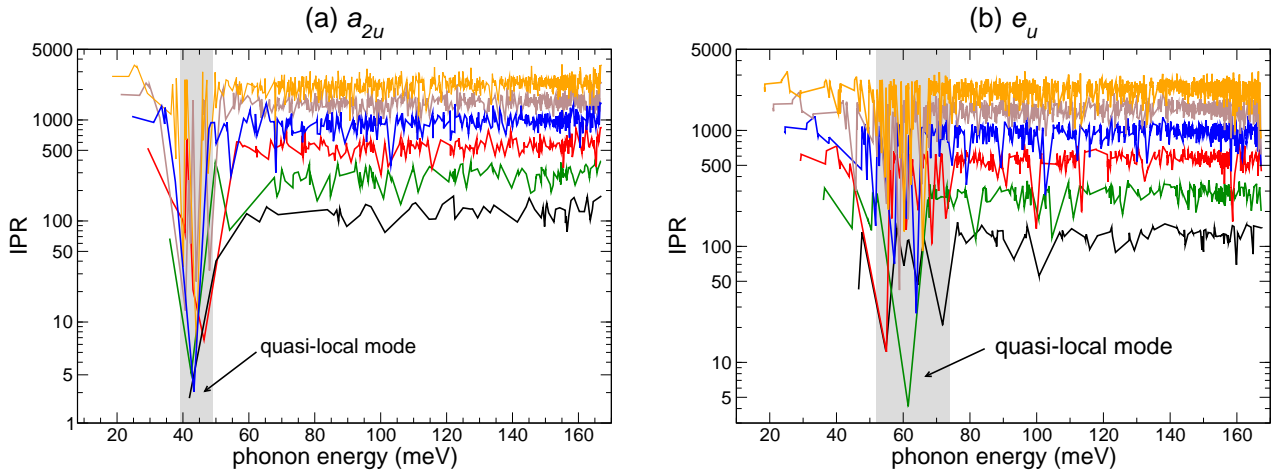


FIG. 3. (a) Inverse participation ratios [Eq. (1)] for a_{2u} symmetry modes for different supercell sizes as a function of energy. (b) Same for e_u modes. Supercells the same as in Fig. 2

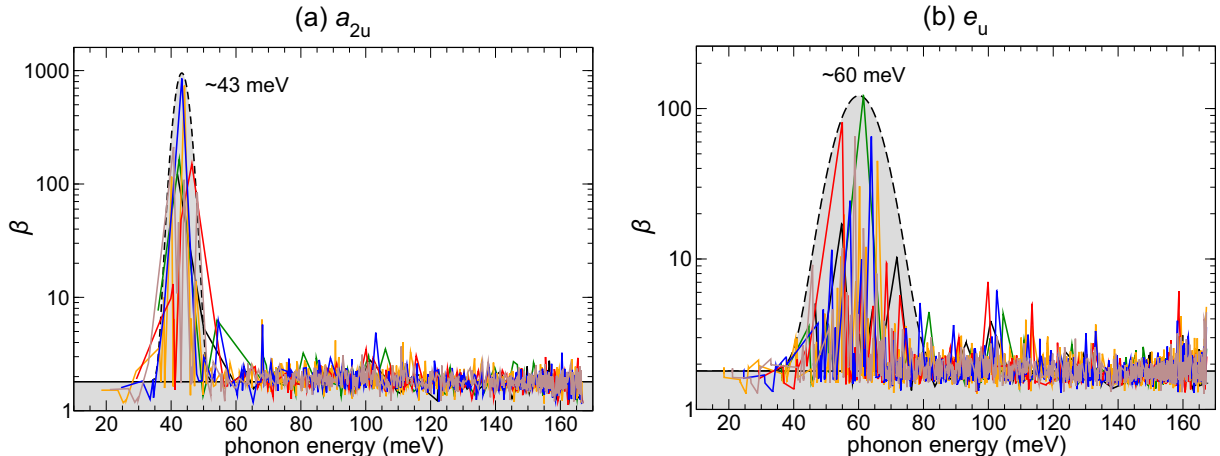


FIG. 4. (a) Localization ratios [Eq. (3)] for a_{2u} symmetry modes for different supercell sizes as a function of energy. The dashed line and shaded region serve as guides to the eye. (b) Same for e_u modes. Note that the y axis has logarithmic scale.

64 meV from the ZPL, shifts with the mass of the silicon isotope as $1/\sqrt{m_{\text{Si}}}$. At low temperatures the phonon sideband in the luminescence spectrum reveals the vibronic structure of the electronic ground state, and thus it is justified to compare experimental results with calculations of the vibrational modes in the ground state. However, in this case we must be very cautious in comparing calculated frequencies of quasi-local vibrational modes with energies of features in the phonon sideband. This is because of a possible complex nature of this phonon sideband. We leave a discussion about comparison of the phonon sideband in luminescence for Sec. V, and here only analyze only the isotopic shifts of vibrations themselves.

In Fig. 5 we present the calculated localization ratios of the a_{2u} vibrational resonance in the energy range 20 – 70 meV for the $5 \times 5 \times 5$ supercell (nominally containing 1000 atoms) for Si isotopes with $m_{\text{Si}} = 28, 29$, and 30 a.u. The calculation with the Si mass of 28 a.u. is the same, as pre-

sented in Fig. 4(a) for the corresponding supercell size. The quasi-local mode has a certain width, meaning that in reality it is made of an infinite number of vibrations with energies around a peak energy of the quasi-local mode. As we deal with finite supercells, this means that for a specific supercell a quasi-local mode splits into a finite number of vibrations. We consider that the vibration for a chosen energy window contributes to the quasi-local mode if its localization ratio is significantly larger than the average localization ratio of all vibrations in the supercell. The criteria ‘‘chosen energy window’’ and ‘‘significantly larger’’ are to some extent arbitrary, and we choose the window 20 – 70 meV and $\beta > 5$, motivated by the results shown in Fig. 4(a). The arbitrariness of the choice is fundamental: it reveals intrinsic difficulties in extracting isotope shifts for broad resonances (both in theory *and* experiment), as discussed below.

For the particular supercell $5 \times 5 \times 5$ we can identify five specific vibrations that contribute to the quasi-

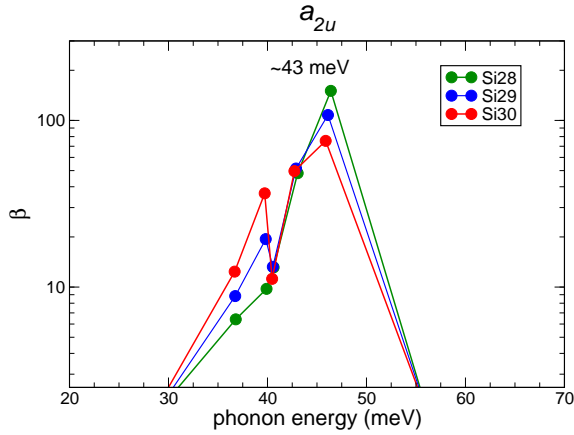


FIG. 5. Localization ratios [Eq. (3)] for the a_{2u} (a) symmetry quasi-local modes around energy 44 meV for three Si isotopes. Calculations performed for the $5 \times 5 \times 5$ supercell.

local mode for all three Si isotopes. The vibration with the largest localization has energies 46.40, 46.11, and 45.88 meV for ^{28}Si , ^{29}Si , and ^{30}Si , respectively. If we were to take these values without any further consideration, we would get isotope shifts $\omega_{28}/\omega_{29} = 1.006$ and $\omega_{28}/\omega_{30} = 1.011$, much smaller than the “ideal” isotope shifts $\sqrt{29/28} = 1.018$ and $\sqrt{30/28} = 1.034$, close to what has been also seen in experiment. However, taking calculated frequencies face value would be valid for a truly localized mode outside the bulk phonon spectrum but is certainly incomplete for a quasi-local mode.

As can be clearly seen in Fig. 5, as we increase the mass of the isotope, two things happen. First, there are shifts of energies pertaining to the individual modes, as we just discussed. Localization (quantified in terms of β) of higher-frequency modes tend to decrease, while local-

TABLE I. Isotopic shifts of the a_{2u} and e_u modes. Ω is the frequency of the resonance [Eq. (4)], and w its width [Eq. (5)].

Supercell	Ω_{28} (meV)	Ω_{29} (meV)	Ω_{30} (meV)	w (meV)
a_{2u}	216	42.28	41.66	1.62
	512	42.90	42.29	2.68
	1000	44.81	43.90	2.48
	1728	43.34	42.79	1.08
	2744	43.03	41.85	2.70
	4096	43.59	42.98	1.67
average	43.33	42.58	41.87	2.04
e_u	216	59.63	58.45	8.46
	512	61.15	60.49	5.20
	1000	58.22	56.81	5.73
	1728	61.14	60.12	6.48
	2744	59.47	58.05	6.46
	4096	60.71	59.06	5.52
average	60.05	58.83	57.70	6.31

ization of lower-frequency modes tend to increase. If we associate β with the weight of the contribution of each specific vibration to the quasi-local mode, we see that there is a re-distribution of weight from the modes with larger energies to the modes with smaller energies. To take this effect into account, we can determine the energy of the quasi-local mode Ω as the weighted average of all the modes that contribute to this resonance:

$$\Omega = \frac{\sum_k \beta_k \omega_k}{\sum_k \beta_k}. \quad (4)$$

While there is freedom in choosing the weight, localization ratio β_k is a first natural choice. If we now weigh the contribution of various modes, we get average energies 44.81, 43.90, and 42.88 meV for the Si isotopes 28, 29, and 30 a.m.u. This now corresponds to isotope shifts $\Omega_{28}/\Omega_{29} = 1.021$ and $\Omega_{28}/\Omega_{30} = 1.045$. One finding is clear: the actual isotope shifts for quasi-local vibrations are different than the estimates based on the analysis of individual vibrational modes. This serves also as a warning about care needed to extract such information from a calculations based on supercells.

We performed a similar analysis for all the considered supercells. The results are shown in Table I. If we average the values obtained for different supercells then we obtain energies 43.32, 42.56, and 41.81 meV for the three Si isotopes. This corresponds to isotopic shifts of $\Omega_{28}/\Omega_{29} = 1.018$ and $\Omega_{28}/\Omega_{30} = 1.035$, very close to the “ideal” isotopic shifts. Since we associate β with the weights of different specific vibrations, we can also define the width w of the quasi-local mode as:

$$w^2 = \frac{\sum_k \beta_k (\omega_k - \Omega)^2}{\sum_k \beta_k}. \quad (5)$$

a_{2u} resonance is very narrow, and its calculated width w is only ~ 2 meV. The width defined above is a qualitative estimate useful to compare different vibrations, but the actual value should of course be taken with some caution.

By reiterating the same procedure for the quasi-local e_u mode we obtain $\Omega_{28}/\Omega_{29} = 1.020$ and $\Omega_{28}/\Omega_{30} = 1.40$, respectively. The results for all the supercells are shown in Table I. Like for the a_{2u} quasi-local mode, isotopic shifts are also close to the “ideal shifts”. The calculated width of the e_u quasi-local mode is $w = 6.3$ meV, thus, larger than for the a_{2u} mode. “Ideal” isotopic shifts for both a_{2u} and e_u modes allow to think of them as representing the motion of an isolated Si-atom inside a hard diamond cage. a_{2u} mode corresponds to vibration along the z axis, while e_u modes correspond to vibrations in the xy plane. Energies and widths of these quasi-local modes (taken as averages over all the considered supercells) are summarized in Table II. The analysis of this Section explain why earlier first-principles calculations of isotope shifts related to quasi-local modes¹² were smaller than the experimental values¹¹. We showed than in order to calculate those shifts one needs to include all the vibrations that contribute to a specific resonance, e.g., via the use of Eq. (4).

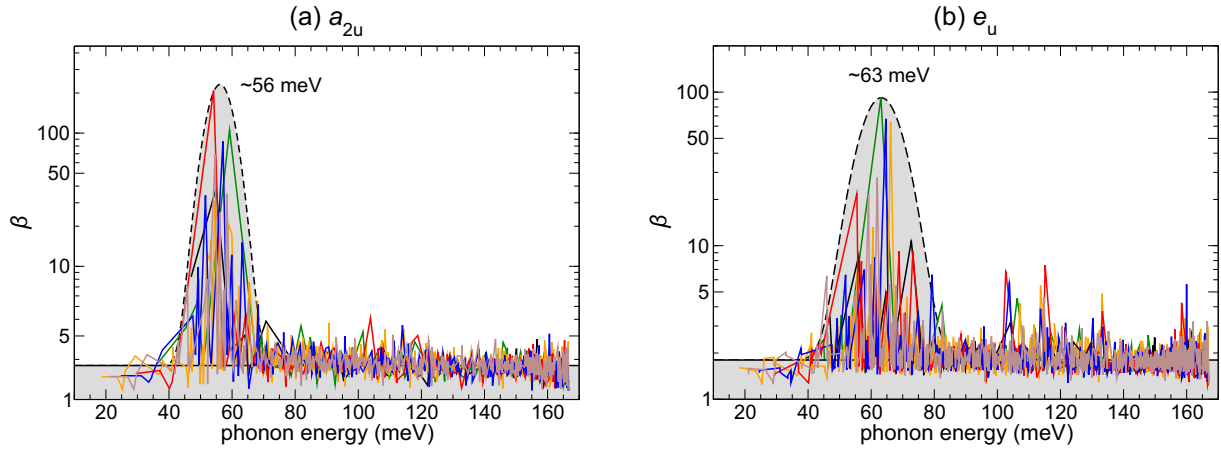


FIG. 6. (a) Localization ratios [Eq. (3)] for a_{2u} (a) and e_u (b) symmetry modes on the excited state for different supercell sizes as a function of energy. The dashed line and shaded region serve as guides to the eye. The y axis has logarithmic scale.

IV. RESULTS: EXCITED STATE

We have performed similar analysis for the vibrational modes in the electronic excited state 2E_u . Regarding all g (even) modes, as well as a_{1u} vibrations, the results are similar to the ground state: there are no quasi-local vibrations. Also similar to the ground state, we find a very pronounced a_{2u} resonance. Calculated localization ratios β are shown in Fig. 6(a). Importantly, the energy of the resonance is 56.3 meV, about 25% larger than in the ground state. Also, the a_{2u} resonance is slightly broader in the excited state with $w = 3.4$ meV, as summarized in Table II. Similar to the ground state, we find a pronounced e_u resonance, as shown in Fig. 6(b). The energy of the resonance is 62.7 meV, thus, only slightly increased with respect to the ground state, and its width, $w = 5.5$ meV, is similar to that in the ground state.

These shifts of vibrational frequencies can be understood from the electronic structure of the SiV($-$) center. The optical excitation corresponds to removing the electron from a more delocalized e_u state to a more localized e_g state⁷. This increases the electron density around the Si atom, and also thus the vibrational frequencies.

V. DISCUSSION

Here, we discuss how our calculations are related to experimental measurements on SiV centers. In a recent PL study¹¹, which was already discussed above, two rather prominent phonon side peaks were observed: a narrow feature (width $w \approx 4 - 5$ meV) at ~ 64 meV from the ZPL and a broad one (width $w > 25$ meV) at ~ 42 meV from the ZPL. As discussed above, a clear isotope shift with respect to the ZPL line of the 64 meV peak was observed. At variance, the 42 meV peak did not show any noticeable change upon isotope substitution. As the authors of the paper admitted¹¹, the lack of apparent change could have been related to difficulties in extract-

ing small differences in energies between broad peaks. It was suggested^{9,11} that the 64 meV mode is a a_{2u} vibration of the Si atom along the symmetry axis, and this vibration is responsible for the 64 meV feature in the PL spectrum.

In addition to shifts of vibronic features, significant isotopic shift of the ZPL energy was found: $\Delta E_{28,29} = E_{28} - E_{29} = 0.36$ meV, and $\Delta E_{28,30} = E_{28} - E_{30} = 0.68$ meV. Typically, such shifts are explained by a difference in vibrational frequencies in the ground and the excited states. At low temperatures zero-point vibrations contribute to the ZPL. As the vibrational frequencies change upon isotope substitutions, so does the ZPL. Experimentally it was found that ZPL shifts to lower energies as the mass of the Si atom increases, and this implies that the vibrational frequencies *on average* are higher in the excited state than in the ground state¹¹. Similarly large isotopic shifts were recently found for the GeV centers in diamond that are similar to SiV centers²⁵.

Let us discuss these experimental findings. Low-temperature luminescence lineshape reveal the vibronic structure in the ground state, so we will first discuss the vibrational modes in the ground state. Like experiment, calculations also indicate the existence of two resonances, one at 43.3 meV and another one at 60.1 meV.

TABLE II. Main results of this work: frequencies Ω and widths w of quasi-local modes (resonances) of a_{2u} and e_u symmetries in the ground and excited states. All results for the ^{28}Si isotope. Average values of frequencies (widths) are given to three (two) significant digits.

State	symmetry	Ω (meV)	w (meV)
Ground state 2E_g	a_{2u}	43.3	2.0
	e_u	60.1	6.3
Excited state 2E_u	a_{2u}	56.2	4.0
	e_u	63.2	6.2

One would be tempted to claim a rather good agreement with experimental values of 42 and 64 meV. However, there is a very large discrepancy concerning the width of these resonances. While calculations indicate that both lower-energy a_{2u} resonance and the higher-energy e_u resonances are narrow (widths w of 2.0 and 6.3 meV, respectively), experiment indicates that the lower-energy resonance is very broad ($w > 25$ meV), and only the higher-energy one is as narrow ($w = 4 - 5$ meV) as theory suggests. Also, in calculations vibrational frequencies of both modes undergo nearly ideal isotope shifts $\sim 1/\sqrt{m_{\text{Si}}}$, while in experiment only the narrow higher-energy peak shows this shift. Two questions arise: 1. Why both peaks are narrow in calculations, but only one in experiment? 2. Is the experimentally observed narrow 64 meV peak a a_{2u} or e_u vibration? Hybrid density functional theory calculations work very well regarding vibrational structure of other defects in diamond, including the NV center^{21,26}, and we should expect it to work well for the SiV center as well. We therefore tentatively suggest that the experimentally observed 64 meV feature in the PL spectrum is in fact the e_u vibration, and not the a_{2u} vibration, as suggested in Ref. 11. In the case of this vibration, the experiment agrees well with calculations regarding (i) the frequency (64 meV vs. 60 meV), (ii) the width (4 – 5 meV vs. 6.3 meV), and (iii) shift of the resonance. We also speculate that the a_{2u} resonance is indeed narrow, but it does not appear in the experimental PL spectrum; the experimental broad feature at 42 meV is in fact not related to quasi-local modes.

Actually, the real question is not why a_{2u} does not appear in the spectrum, but why is the e_u resonance visible at all. Optical transition is between states 2E_u (excited) and 2E_g (ground). Thus, according to the group-theoretical analysis, in the Franck-Condon approximation one should expect to see only the even-symmetry a_{1g} phonons. However, density functional calculations indicate the presence of the (weak) Jahn-Teller effect both in the excited and the ground state⁷, leading to lowering of the symmetry to C_{2h} . Since symmetry-lowering retains inversion symmetry, this indicates Jahn-Teller coupling to e_g phonons both in the ground ($E_u \otimes e_g$ JT system) and the excited ($E_g \otimes e_g$ JT system) states. Optical transition between these two JT systems should again involve only even-symmetry (g) phonons, leaving the appearance of the e_u mode in the experiment unexplained.

Table II shows that frequencies of a_{2u} and e_u phonons in the excited state are rather close to each other. Keeping in mind finite width of these resonances, there is some overlap in energies. Any small perturbation, such as quadratic interactions²⁷ or strain, could then mix these vibrations. If this is the case, one could expect to see the signatures of both a_{2u} and e_u vibrations in the emission spectrum. However, it remains unclear how such interaction could lead to the situation where only e_u vibration appears, while a_{2u} vibration does not. One more option is provided by the Herzberg-Teller effect, whereby the transition dipole moment is modulated by the vibration²⁷.

When the vibration is of a_{2u} symmetry, this reduces the instantaneous symmetry of our system from D_{3d} to C_{3v} . However, degeneracy of electronic states is not removed. At variance, e_u vibration would reduce the symmetry to C_1 , removing the degeneracy and possibly leading to a appreciable modulation of the transition dipole moment. While the appearance of unsymmetric modes in optically allowed transitions is very unusual²⁷, we do not reject this possibility. However, the study of optical transitions and the luminescence lineshape of SiV centers is beyond the aim of the present work and requires further work. Understanding the mechanism of the vibronic coupling at SiV centers will be also pivotal in explaining experimentally measured polarization of the phonon side-band⁹.

Finally, we discuss the experimentally observed isotope shift of the ZPL¹¹. Our results show that the vibrational frequencies of quasi-local modes are indeed higher in the excited state than in the ground state. As discussed above, this would lead to lowering of the ZPL upon substitution with heavier Si atoms, in complete agreement with experiments. If we first assume that all of the shift is due to quasi-local modes, we could estimate the change of the ZPL when ^{28}Si is replaced by ^{29}Si as

$$\Delta E_{28,29} \approx \frac{1}{2}\hbar(\Omega_{a_{2u}}^e + 2\Omega_{e_u}^e - \Omega_{a_{2u}}^g - 2\Omega_{e_u}^g) \times \left(1 - \sqrt{\frac{m_{28}}{m_{29}}}\right). \quad (6)$$

Estimate yield a value of 0.17 meV, almost twice smaller than the experimental value of 0.36 meV. Similarly, the calculated value for $\Delta E_{28,30}$ of 0.32 meV is smaller than the experimental one of 0.68 meV. We could alternatively calculate the shift by including the contribution of all phonons. For this purpose, we can determine the contribution of zero-point vibrations to the energies of excited and ground states as:

$$E_{\text{ZPV}} = \frac{1}{2} \sum_i \hbar\omega_i^e - \frac{1}{2} \sum_i \hbar\omega_i^g. \quad (7)$$

The sum converges very fast as a function of the supercell size, and we obtain values 17.06 meV for ^{28}Si , 16.80 meV for ^{29}Si , and 16.56 meV for ^{30}Si . This gives $\Delta E_{28,29} = 0.26$ meV and $\Delta E_{28,30} = 0.50$ meV. These results are much closer to the experimental values. We believe that to explain the remaining discrepancy one would need to consider the above-mentioned Jahn-Teller effect, in which the zero-point vibrational contributions differ from the one given in Eq. (7).

VI. SUMMARY AND CONCLUSIONS

In summary, we have studied vibrational spectrum of the negatively charged silicon-vacancy center in diamond by first-principles density functional theory calculations. The electronic structure, geometry, and force constants were calculated with the hybrid density functional of

Heyd, Scuseria, and Ernzerhof. The vibrational spectrum of the defect was modeled in large supercells containing up to 4096 atoms (nominal size) using the embedding procedure whereby the dynamical matrix of a large supercell was constructed from the dynamical matrix of a defect in a 216-atom supercell and the dynamical matrix of bulk diamond. This is possible because the interaction of atoms in diamond is rather short-ranged, even in the case of charged defects. We find that vibrations that all even-symmetry (a_{1g} , a_{2g} , and e_g), as well a_{1u} vibrations are essentially slightly perturbed bulk modes. However, we find very pronounced quasi-local modes of a_{2u} and e_u modes that correspond to the vibration of the Si atom along and perpendicular to the defect symmetry axis, respectively. We have presented the methodology to calculate isotope shifts of these modes, and find excellent agreement with experiment. We have also found that the vibrational frequencies in the electronic excited state are larger than in the ground state, also in full agreement with experimental findings. Finally, we tentatively suggested that the experimental observed feature in the photoluminescence spectrum at 64 meV is a quasi-local e_u mode. While the appearance of this feature in the ex-

perimental spectrum remains unexplained, we provided some possible physical mechanisms of vibronic coupling. By systematically addressing the vibrational properties of the SiV center, our work will be helpful in understanding physical properties of single-photon emitters in diamond and other materials.

ACKNOWLEDGMENTS

We thank M. Bijeikyté, M. W. Doherty, F. Jelezko, I. S. Osad'ko, and L. Razinkovas for fruitful discussions. A. G. acknowledges the support from NIIF Supercomputer Center Grant No. 1090, and National Research Development and Innovation Office of Hungary (NKFIH) within the Quantum Technology National Excellence Program (Project No. 2017-1.2.1-NKP-2017- 00001). A. A. was supported by a grant No. MERA.NET-1/2015 from the Research Council of Lithuania. Additional calculations were performed at the High Performance Computing Center “HPC Saulėtekis” in Faculty of Physics, Vilnius University.

-
- * gali.adam@wigner.mta.hu
 † audrius.alkauskas@ftmc.lt
- ¹ G. Davies, *Rep. Prog. Phys.* **44**, 787 (1981).
- ² L. Gordon, J. R. Weber, J. B. Varley, A. Janotti, D. D. Awschalom, and C. G. Van de Walle, *MRS Bulletin* **38**, 802807 (2013).
- ³ E. Neu, D. Steinmetz, J. Riedrich-Möller, S. Gsell, M. Fischer, M. Schreck, and C. Becher, *New J. Phys.* **13**, 025012 (2011).
- ⁴ A. Sipahigil, K. D. Jahnke, L. J. Rogers, T. Teraji, J. Isoya, A. S. Zibrov, F. Jelezko, and M. D. Lukin, *Phys. Rev. Lett.* **113**, 113602 (2014).
- ⁵ L. J. Rogers, K. D. Jahnke, M. H. Metsch, A. Sipahigil, J. M. Binder, T. Teraji, H. Sumiya, J. Isoya, M. D. Lukin, P. Hemmer, and F. Jelezko, *Phys. Rev. Lett.* **113**, 263602 (2014).
- ⁶ J. P. Goss, R. Jones, S. J. Breuer, P. R. Briddon, and S. Öberg, *Phys. Rev. Lett.* **77**, 3041 (1996).
- ⁷ A. Gali and J. R. Maze, *Phys. Rev. B* **88**, 235205 (2013).
- ⁸ C. Hepp, T. Müller, V. Waselowski, J. N. Becker, B. Pingault, H. Sternschulte, D. Steinmüller-Nethl, A. Gali, J. R. Maze, M. Atatüre, and C. Becher, *Phys. Rev. Lett.* **112**, 036405 (2014).
- ⁹ L. J. Rogers, K. D. Jahnke, M. W. Doherty, A. Dietrich, L. P. McGuinness, C. Müller, T. Teraji, H. Sumiya, J. Isoya, N. B. Manson, and F. Jelezko, *Phys. Rev. B* **89**, 235101 (2014).
- ¹⁰ H. Sternschulte, K. Thonke, R. Sauer, P. C. Münzinger, and P. Michler, *Phys. Rev. B* **50**, 14554 (1994).
- ¹¹ A. Dietrich, K. D. Jahnke, J. M. Binder, T. Teraji, J. Isoya, L. J. Rogers, and F. Jelezko, *New J. Phys.* **16**, 113019 (2014).
- ¹² J. P. Goss, P. R. Briddon, and M. J. Shaw, *Phys. Rev. B* **76**, 075204 (2007).
- ¹³ L. J. Rogers, K. D. Jahnke, T. Teraji, L. Marseglia, C. Müller, B. Naydenov, H. Schauffert, C. Kranz, J. Isoya, L. P. McGuinness, and F. Jelezko, *Nature Comm.* **5**, 4739 (2014).
- ¹⁴ G. Kresse and J. Hafner, *Phys. Rev. B* **47**, 558 (1993).
- ¹⁵ A. V. Krukau, O. A. Vydrov, A. F. Izmaylov, and G. E. Scuseria, *J. Chem. Phys.* **125**, 224106 (2006).
- ¹⁶ J. P. Perdew, K. Burke, and M. Ernzerhof, *Phys. Rev. Lett.* **77**, 3865 (1996).
- ¹⁷ C. Freysoldt, B. Grabowski, T. Hickel, J. Neugebauer, G. Kresse, A. Janotti, and C. G. Van de Walle, *Rev. Mod. Phys.* **86**, 253 (2014).
- ¹⁸ J. Slater, *The Self-consistent Field for Molecules and Solids. Quantum Theory of Molecules and Solids*, Vol. 4 (McGraw-Hill, 1965).
- ¹⁹ B. Kaduk, T. Kowalczyk, and T. Van Voorhis, *Chem. Revs.* **112**, 321 (2012).
- ²⁰ A. Gali, E. Janzén, P. Deák, G. Kresse, and E. Kaxiras, *Phys. Rev. Lett.* **103**, 186404 (2009).
- ²¹ A. Alkauskas, B. B. Buckley, D. D. Awschalom, and C. G. Van de Walle, *New J. Phys.* **16**, 073026 (2014).
- ²² L. Landau and E. Lifshitz, *Quantum Mechanics*, 3rd ed. (Pergamon, 1977).
- ²³ R. J. Bell, P. Dean, and D. C. Hibbins-Butler, *J. Phys. C: Solid State Phys.* **3**, 2111 (1970).
- ²⁴ M. C. M. O'Brien, *J. Phys. C: Solid State Phys.* **5**, 2045 (1972).
- ²⁵ E. A. Ekimov, V. S. Krivobok, S. G. Lyapin, P. S. Sherin, V. A. Gavva, and M. V. Kondrin, *Phys. Rev. B* **95**, 094113 (2017).
- ²⁶ A. Gali, T. Simon, and J. E. Lowther, *New Journal of Physics* **13**, 025016 (2011).
- ²⁷ I. S. Osad'ko, *Sov. Phys. Uspekhi* **22**, 311 (1979).